Finite Element Investigation on Shear Lag in Composite Concrete-Steel Beams with Web Openings

Dr. Rafa'a Mahmood Abbas
Lecturer
College of Engineering-University of Baghdad
rafaamaa@yahoo.com

Hayder Jaber Shakir
M.Sc. Student
College of Engineering-University of Baghdad
hayder_civil_1988@yahoo.com

ABSTRACT

In this paper, effective slab width for the composite beams is investigated with special emphasis on the effect of web openings. A three dimensional finite element analysis, by using finite element code ANSYS, is employed to investigate shear lag phenomenon and the resulting effective slab width adopted in the classical T-beam approach. According to case studies and comparison with limitations and rules stipulated by different standards and codes of practice it is found that web openings presence and panel proportion are the most critical factors affecting effective slab width, whereas concrete slab thickness and steel beam depth are less significant. The presence of web opening reduces effective slab width by about 21%. Concentrated load produces smaller effective slab width when compared with uniformly distributed and line loads. Generally, standard codes of practice overestimate effective slab width for concentrated load effect, while underestimate effective slab width for uniformly distributed and line load effect. Based on the data available, sets of empirical equations are developed to estimate the effective slab width in the composite beams with web openings to be used in the classical T-beam approach taking into account the key parameters investigated.

Key words: composite beam, shear lag, effective slab width, web openings, finite element

التحري بطريقة العناصر المحددة لتخلف القص في العتبات المركبة من الفولاذ والخرسانة بوجود فتحات في وترة الروافد الفولاذية

د.رافع محمود عباس
مدرس
كلية الهندسة-جامعة بغداد

حيدر جابر شاكر
طالب ماجستير
كلية الهندسة-جامعة بغداد

الخلاصة

تم في هذا البحث اجراء دراسة تاثير وجود الفتحات في وترة الروافد المركبة من الفولاذ والخرسانة على العرض الفعال للشفة الخرسانية. تم عمل نماذج ثلاثية الابعاد بطريقة العناصر المحددة, باستعمال برنامج التحليل الجاهز ANSYS, للتحقق من ظاهرة تخلف القص والعرض الفعال للشفة الخرسانية الناتج عنها. بينت نتائج هذه الدراسة والمقارنة مع متطلبات ومحددات المراجع والمدونات القياسية ان تاثير وجود فتحات في وترة الروافد الفولاذية ونسبة ابعاد البلاطة الخرسانية هي اهم العوامل المؤثرة على العرض الفعال للشفة الخرسانية وبدرجة اقل يؤثر سمك البلاطة الخرسانية وعمق الرافدة الفولاذية. ان وجود فتحات في وترة الروافد الفولاذية يقلل العرض الفعال بمقدار 21% وان العرض الفعال للشفة الخرسانية بسبب الاحمال المركزة هو اقل مما في حالة الاحمال المنتظمة او الاحمال الخطية. وبشكل عام, فان المدونات القياسية تبالغ في تقدير العرض الفعال الناتج عن الاحمال المركزة وتقلل من تقديره في حالة الاحمال المنتظمة او الاحمال الخطية. واستنادا الى البيانات

المتوفرة تم اقتراح علاقات رياضية مبسطة تساعد المصمم على احتساب العرض الفعال للبلاطة في العتبات المركبة ذات الفتحات بصورة مباشرة من خلال بعض المتغيرات التي تمت دراستها.

كلمات الرئيسية: العتبات المركبة، تخلف القص، عرض السقف الفعال، فتحات في وترة الروافد، تحليل العناصر المحددة

1. INTRODUCTION

A typical form of composite construction, such as a floor within a building or a bridge deck, consists of a slab connected to a number of parallel beams. It is valid in principle to divide the system into a series of T-beams, the slab width obtained from such a simple division may not be fully effective in resisting the compressive forces from bending. The transmission of shear from the connectors on top flange of the steel beam to the slab becomes less effective as the beam spacing increase. Higher shear is induced near the beam, but falls off towards the center line between two beams. Under the action of the axial compression and eccentric edge shear flows, the flange distorts and does not compress as assumed in simple beam theory with plane sections remaining plane. The amount of distortion depends on both the shape of the flange in plane and on the distribution of shear flow along its edge. A narrow flange distorts little and its behavior approximates what is assumed in simple beam theory. In contrast, the wide flanges distort seriously because the compression induced by the edge shears does not flow very far from the loaded edge, and much of each wide flange is ineffective. The decrease in flange compression away from the loaded edge due to shear distortion is called shear lag.

The longitudinal compressive stresses at top of the slab have a non-uniform distribution, as shown in **Fig.1**. In order that the T-beam approach can be used, a reduced value of the width of the slab, termed effective width, is therefore used in design and analysis. It is defined as that width of slab that, when acted on uniformly by the actual maximum stress, would have the same static equilibrium effects as the existing variable stress. The effective width is affected by various factors such as the type of loading, the boundary conditions at the supports, and the ratio of beam spacing to span.

Eq. (1) is generally used to calculate the effective slab width in composite beams , **Heins, 1976.**

$$2\overline{b} = \frac{2\int_0^b \sigma_z \, dx}{(\sigma_z)_{max}} \qquad (1)$$

Where $(2\bar{b})$ is the effective width of the concrete slab, (b) is a half slab width, (σ_z) represents the normal stress in the longitudinal direction in the slab at top surface, and $(\sigma_z)_{max}$is the maximum normal stress between $0 \leq x \leq b$.

2. BACKGROUND

In **2003**, **Fragiacomo, and Amadio** performed experimental tests for the evaluation of the effective width for elastic and plastic analysis of steel-concrete composite beams with both cases of sagging and hogging bending moments. It was shown that for all specimens the effective width increases with the load, approaching the width of whole slab near the collapse. In zones of sagging bending moment, because of the limited ductility and brittle rupture of concrete, it was suggested to keep the conservative equation proposed by the Eurocode-4 for evaluating the quantity of the effective slab width to (l_o/8). In the zones of hogging bending moment, because of the high ductility of the reinforcing bars, a less conservative solution was proposed to (l_o/4), where (l_o) is the distance between the points of zero bending moment.

Chiewanichakorn, 2004, introduced an effective slab width definition through a three-dimensional non-linear finite element analysis employed to evaluate and determine the actual effective slab width of steel-composite bridge girders. The resulting effective width was larger than the ones provided by many design specifications, both nationally and internationally. The revised effective slab width criteria based on the proposed effective slab width definition was compared with other design specifications, specifically AASHTO LRFD, British, Canadian, Japanese, and Eurocode-4 design specifications.

Chun, and Cai, 2008, investigated the shear-lag phenomenon in steel-concrete composite floor model in both elastic and inelastic stages through experimental study. The model consisted of three identical longitudinal girders and two transverse girders at the ends of the longitudinal girders. Each of the three longitudinal girders was subjected to sagging moments through four-point loads. The tested beams were analyzed by finite element method through ANSYS program. It was found that the effective slab width at the ultimate strength is larger than that at the serviceability stage. The ratio of slab width to span length and loading types has significant influence on the degree of shear lag. The shear-lag effect is more obvious under one-point load than other loading types. **Salama and Nassif, 2011,** presented results from an experimental and analytical investigation to determine the effective slab width in steel-concrete composite beams. Beam test specimens had variable flange widths, steel beam sizes and various degrees of composite action. It was observed that the increase of the aspect ratio from 0.25 to 0.75 decreases the effective width ratio about 15%. Also it was observed that the stress distribution for the beams does not change as the depth of steel beams increases.

3. EFFECTIVE WIDTH IN CODE OF PRACTICE

The effective width can be thought of as the width of theoretical flange, which carries a compression force with uniform stress of magnitude equal to the peak stress at the edge of the prototype wide flange when carrying the same total compression force. The effective width concept has been widely recognized and implemented into different codes of practice around the world. The formulas used by various codes are shown in **Table 1**.

4. OBJECTIVE

The aim of this study is to investigate the behavior of the effective slab width and stress distribution (shear lag) on the composite beams with web openings subjected to static load. The composite beams are consisting of a concrete slab connected together with a steel beam by means of headed stud shear connector. The openings are made in the steel section. Three-dimensional finite element model by ANSYS 11.0 program is used for simulating the behavior of composite steel-concrete members within linear elastic range of the behavior of composite beam. The composite beams are analyzed by considering linear behavior of steel beam, concrete slab, shear connectors, and slab reinforcement.

5. VERIFICATION OF THE FINITE ELEMENT IDEALIZATION

The validity and accuracy of the finite element idealization are studied and checked by analyzing Steel-concrete composite beams that have been experimentally tested by **Hamoodi and Hadi, 2011**. Six composite beams of steel I-section and concrete slab connected together by headed shear studs welded to the top flange of the steel section are tested. Each one has an overall length of 2.1m and a clear span of 2.0m and subjected to a concentrated load at mid span. The dimensions and reinforcement details of a typical beam section are shown in **Fig.2**

In the present section, two types of composite beam are chosen, one solid beam without web opening designated as beam (CB0), and beam (CB3) with two web openings. The solid beam (CB0) is chosen to demonstrate the behavior of a typical composite beam and to represent a reference beam when web openings are introduced. The second beam (CB3) is chosen to demonstrate the behavior of composite beam when constructed with openings in the web and to verify finite element idealization with experimental one when openings are present in the web of the steel beam. The configurations of the six tested beams by **Hamoodi and Hadi, 2011** are shown in **Fig.3**.

5.1 Finite Element Modeling and Material Properties

The steel-concrete composite beams are modeled by a three-dimensional eight-node solid element (SOLID 45) is used for the concrete slab, while the steel reinforcement bar is modeled by a spar element (LINK 8). In the modeling of the steel beam; a four-node shell element (SHELL63) is used. A spar element (LINK8) is used to model shear connector to resist uplift, while the dowel action of shear connector is modeled by combine element (COMBIN14). In the modeling of the interface between two surfaces a contact element (CONTA174) and target element (TARGE170) are used. Material properties of the two beams are summarized in **Table 2**. The boundary conditions of these beams are applied to roller and hinged support as shown in **Figs.4 and 5**. The external force is (80kN) modeled as point loads distributed across the concrete slab that is located over the steel section at mid-span.

5.2 Verification of the Results

A comparison between the numerical and the experimental results has been made to verify the accuracy of the numerical models obtained using linear finite element analysis carried out on beams CB0 and CB3. **Tables 3** and **4** show the comparison between experimental and analytical deflection, while experimental and analytical load-deflection curves are shown in **Figs.6** and **7**. From the comparison presented it can be concluded that the adopted finite element idealization and the resulting numerical beam model are adequate and yield results which are accurate and in close agreement with experimental one.

6. PARAMETRIC STUDY

Several important parameters affecting the stress distribution in the concrete slab, and hence the effective slab width for the composite beams with web openings, are investigated using the presently verified FE model. One parameter has been considered to vary while the other parameters being held constant in order to separate the effect of the parameter considered. The simply supported composite beams tested by **Hamoodi and Hadi, 2011,** have been selected to carry out the parametric study. The parameters, which have been studied, can be summarized as follows:

1. Effect of openings location, size and number.
2. Effect of beam slab width to span length ratio (2b/L ratio).
3. Effect of concrete slab thickness.
4. Effect of boundary conditions at the edges of the concrete slab.
5. Effect of steel beam depth.

In this work, three types of loading are investigated:

- Concentrated Load (CL) at mid span (80 kN).
- Line Load (LL) on the longitudinal web axis (40 kN/m).
- Uniform Distributed Load (UDL) on over all slab equivalents to (80 kN).

6.1 Effect of Openings Location, Size and Number

In this section, a comparison is presented between results of beam CB0, a composite beam without web openings, and results of beams CB1 and CB2, composite beams with single central and quarter span opening, respectively, in order to investigate the effect of openings location. Results presented in **Fig.8** shows that introducing a central opening causes an increase by about 26.60% in the slab longitudinal stresses at mid-span section due to CL, while an increase by about 18.8% is observed when a single web opening is introduced at quarter-span section. On the other hand, **Fig.9** indicates that introducing a central web opening causes a maximum decrease of about 21% in the effective slab width at mid-span section, while a maximum decrease of about 18% due to the presence of a single quarter-span section is observed.

The effect of increasing the number of web openings is presented through a comparison between results of beam CB3, a beam with two openings, and results of beam CB4, a beam with three openings. Results presented in **Fig.10** shows that increasing the number of openings from two to three causes a maximum increase in the mid-span section longitudinal slab stresses of about 19% due to CL loading, whereas a maximum decrease in the effective slab width of about 6% at mid-span section is observed when comparing results in **Fig.11** due to increasing number of web openings.

The effect of size of web openings is shown in comparison between results of beam CB4, a beam with (100mm) opening depth and (200mm) width, and results of beam CB5, a beam with (80mm) opening depth and (100mm) width. Results presented in **Fig.12** shows that decreasing the web opening size causes a decrease of about 10% in the slab longitudinal stresses at mid span section due to CL loading. On the other hand, a minor effect for the web opening size on the effective slab width near mid span can be concluded when comparing results presented in **Table 6** for beams CB4 and CB5 for the three types of loadings. The summary on the effect of openings location, size and number on the effective width ratio at mid-span for the six beams and for the three types of loadings is listed in **Table 5**. Comparison of the effective slab width with design specifications is shown in **Table 6**.

6.2 Effect of Beam Slab Width to Span Length Ratio (2b/L ratio)

The effect of panel proportion on the effective slab width at mid-span for beams CB3 and CB4 for the three types of loading is listed in **Table 7**. Comparison of the effective slab width with design specifications is shown in **Table 8**. It can be seen that the maximum effect for uniformly distributed load situation occurs when the panel proportion increases from (0.25) to (0.50) the maximum slab top surface stress decreases by 33%, and 27% for beams CB3 and CB4 as shown in **Figs. 13** and **14** , respectively. The maximum effect of panel proportion on effective slab width occurs under concentrated load and line load situations for beams CB3 and CB4, respectively. When the panel proportion increases from (0.25) to (0.50) the effective slab width decreases by 11.30% and 10% for beams CB3 and CB4, respectively as shown in **Figs. 15** and **16**.

6.3 Effect of Concrete Slab Thickness

The effect of varying slab thickness on the effective slab width at mid-span for beams CB3 and CB4 for the three types of loading is listed in **Table 9**. Comparison of the effective slab width with design specifications for the three values of the slab thickness is shown in **Table 10**. From the obtained results it can be seen that the maximum effect occurs under concentrated load situation. When the slab thickness increases from (60mm) to (120mm), the maximum slab top surface stress decreases by 31%, and 40% for beams CB3 and CB4, respectively as shown in **Figs. 17** and **18**, whereas the maximum effect of varying slab thickness on the effective slab width occurs under line

load and concentrated load situations for beams CB3 and CB4, respectively. When the slab thickness increases from (60mm) to (120mm), the effective slab width decreases by 10.40% and increases by 4.50% for beams CB3 and CB4, respectively as shown in **Figs.19** and **20**.

6.4 Effect of Boundary Conditions at the Edges of the Concrete Slab

The aim of this section is to investigate the effect of concrete slab continuity along longitudinal and transverse edges as in actual floor and roof systems on the effective slab width and stress distribution in the slab due to different types of loading and panel proportions. The proposed modeling for slab continuity in the finite element model is simulated by artificial boundary conditions applied along slab edges by providing vertical rollers along these edges and across concrete slab depth as shown in **Fig. 21**.

The results of the effect of slab boundary condition with three values of panel proportions on the effective slab width at mid-span for beams CB3 and CB4 due to three types of loading are listed in **Table 11**. Comparison of the effective slab width with design specification is shown in **Table 12**. From the obtained results, it can be seen that the maximum effect for uniformly distributed load situation occurs when the panel proportions increase from (0.25) to (0.50), the maximum slab top surface stress decreases by 30%, and 25% for beams CB3 and CB4, respectively as shown in **Figs. 22 and 23**. The maximum effect of panel proportion on the effective slab width under concentrated load situation occurs when the panel proportions increase from (0.25) to (0.50), the effective slab width decreases by 11% and 21% for beams CB3 and CB4, respectively as shown in **Figs. 24 and 25**. The results also show a comparison between continuous and discontinuous slabs. Applying the boundary condition to the edge of slab makes an increase in slab top surface stress about 3% and 4% for beams CB3 and CB4, respectively under the uniformly distributed load situation for panel proportion (0.50) and has a minor effect on concentrated load and line load situations. The maximum effect on effective slab width occurs under line load and uniform distributed load for beams CB3 and CB4, respectively. Applying the boundary condition increases the effective slab width by about 7% for beam CB3 with panel proportion of (0.25) and by 2% for beam CB4 with panel proportion (0.50).

6.5 Effect of Steel Beam Depth

The effect of varying steel beam depth on the effective slab width at mid-span for beams CB3 and CB4 for the three types of loading is listed in **Table 13**. Comparison of the effective slab width with design specifications is shown in **Table 14**. From the obtained results, it can be seen that the maximum effect under the uniformly distributed load situation occurs when the steel beam depth increases from (160mm) to (240mm), the maximum slab top surface stress decreases by 42% for both beams CB3 and CB4 as shown in **Figs. 26** and **27**. The maximum effect of varying steel beam depth on the effective slab width under concentrated load situation for both beams CB3 and CB4 occurs when the steel beam depth increases from (160mm) to (240mm), the effective slab width decreases by 13% and 11% for beams CB3 and CB4, respectively as shown in **Figs. 28** and **29**.

7. PROPOSED EFFECTIVE SLAB WIDTH EQUATIONS

The current parametric study provides a database for the effective slab width for composite steel-concrete beams with web openings. This database can be used to develop expressions for the effective slab width. The results presented previously show that web openings location and type of loading on the beam are the most critical factors affecting effective slab width values. Uniformly distributed load and line load generally yields close values for the effective slab width. Therefore, it is suggested to treat both loading type in a uniform manner such that single equation based on

uniform load data is adopted. Accordingly, it is intended to provide two sets of equations, one for the case when central span web opening exists and the other for the case of quarter span opening. Moreover, each set consists of two equations, one for effective slab width due to concentrated load effect and the other due to uniform distributed load effect.

Proposed equations include the three major parameters that affect effective slab width ($2\bar{b}$), which are panel width to span length ratio (2b/L ratio), slab thickness (t_{slab}) and steel beam depth (h_{steel}) as shown below:

- **Quarter-span openings**

1. Concentrated Load *:*

$$2\bar{b} = 177.4 + 978.2\,(2b/L) - 0.15\,(t_{slab}) - 0.63\,(h_{steel}) \quad (2)$$

2. Uniformly Distributed and Line Loads:

$$2\bar{b} = -13.9 + 1864.4(2b/L) - 0.24(t_{slab}) - 0.023(h_{steel}) \quad (3)$$

- **Mid-span openings**

3. Concentrated Load*:*

$$2\bar{b} = 106.2 + 964.9(2b/L) + 0.22\,(t_{slab}) - 0.44(h_{steel}) \quad (4)$$

4. Uniformly Distributed and Line Loads *:*

$$2\bar{b} = 40.8 + 1643.3(2b/L) + 0.29\,(t_{slab}) - 0.11(h_{steel}) \quad (5)$$

In these equations, L is span length (mm), b half slab width (mm), t_{slab} is concrete slab thickness (mm) and h_{steel} is steel beam depth (mm).

Finally, it is proposed to present another set of equations that correlate effective slab width with the most critical factor obtained from the parametric study, i.e., panel aspect ratio (2b/L). These equations take into account implicitly the effect of web opening presence while ignoring concrete slab thickness and steel beam depth. This set of equations is intended to be more simplified than the previously presented equations and more convenient to be used by design authorities and building codes.

Considering that; (S=2b) as in the design codes and panel aspect ratio β= (2b/L), then the effective slab width equations:

1. Due to Concentrated Load:

$$2\bar{b} = (0.7 - 0.3\beta) \times S \quad (6)$$

2. Due to Uniformly Distributed and Line Loads:

$$2\bar{b} = (1.0 - 0.3\beta) \times S \quad (7)$$

These equations take into account the effect of span length (L) and spacing of the beams (S) as stipulated by various codes presented in **Table 1**.

8. VERIFYING PROPOSED EQUATION RESULTS

To verify the validity of the proposed equations, comparison was made between the results obtained from the developed equations and the results from the current finite element analysis. **Figs.30-35** show plots of the comparison of the effective slab width ($2\bar{b}$) obtained from the finite element analysis and those obtained from Eqs. (2), (3), (4), and (5) for the three types of loading. **Figs.36** and **47** show plots of the comparison of the effective slab width ($2\bar{b}$) obtained from the finite element analysis and those obtained from the simplified Eqs. (6) and (7). It can be observed that the proposed equations have good agreement with the finite element results which indicates that the proposed equations have good correlation with numerical result.

9. CONCLUSIONS

An extensive study is carried out on the behavior of composite steel-concrete beams in which the upper flange of the steel beam is attached to reinforced concrete slab. Stress distribution and effective slab width for the composite beams are investigated with special emphasis on composite beams with openings in the steel web. The finite element analysis has been used to investigate shear lag phenomenon and the resulting effective slab width adopted in the classical T-beam approach. Comparison is made with available limitation and regulations stipulated by different codes of practice. According to the case studies and comparison presented in this study, the following conclusions are drawn:

1. The results presented show that the effective slab width strongly depends on the type of loading with the minimum values obtained due to concentrated load, while uniformly distributed load and line load generally yield similar values approaching full slab width.
2. For the different types of loading considered, effective slab width depends on the position along the span of the beam. Effective slab width is reduced to minimum values near mid span, support and opening locations, while it tends to reach full slab width elsewhere.
3. Introducing central span web opening causes a maximum decrease in the effective slab width of about 21%, whereas a maximum decrease of about 18% is observed due to presence of quarter span web opening.
4. Increasing the number of web openings has a minor effect on the effective slab width with a maximum decrease of 6% at mid span section observed when the number of openings is increased from two to three.
5. Varying standard web opening size has negligible effect on the effective slab width.
6. Increasing steel beam depth to twice values causes a decrease in the effective slab width of about 11% to 13% for different web opening configurations. Almost the same effect is observed when concrete slab thickness is increased twice.
7. Results indicate that the standard codes of practice, and hence the T-beam theory, generally overestimate the effective slab width due to concentrated loads especially for small values of panel proportions, i.e., 2b/L=0.25. On the other hand, close agreement is observed for higher panel aspect ratios.
8. Uniformly distributed load and line load results reveal that the standard codes of practice and the T-beam theory underestimate the effective slab width especially for high values of panel proportion, i.e., 2b/L=0.50. On the other hand, close agreement is observed for smaller panel aspect ratios.
9. Sets of empirical expressions to estimate effective slab width are developed. These equations can be used to estimate effective slab width for different types of loading, web opening locations, panel proportion, concrete slab thickness and steel beam depth.

REFRERENCES

- ANSYS 11.0 Inc., 2002, *ANSYS Manual*, Version 11.0, U.S.A.
- American Concrete Institute, 2008, *Building Code Requirements for Structural Concrete*, ACI-318M-08, Detroit, Michigan, USA.
- AASHTO-LRFD, 2004, *Bridge Design Specification*, American Association of State Highway and Transportation Officials (AASHTO), Third Edition, Washington D.C.
- AISE, 1986, *Load Resistance Factor Design (LRFD)*, Manual of Steel Construction, First Edition, American Institute of Steel Construction, pp.1124.
- BSI, 1997, *Structure Use of Concrete, Part 1: Code of Practice for Design and Construction*, BSI8110, British Standard Institution, London.
- Chiewanichakorn**,** M., and Chen, S. S., 2004, *Effective Flange Width Definition for Steel-Concrete Composite Bridge Girder*, Journal of Structure Engineering, ASCE, Vol.130, No. 12, pp.2016-2031.
- Chun-Yu Tian, and Cai, C. S., 2008, *Effective Width of Steel-Concrete Composite Beam at Ultimate Strength State*, Journal of Engineering Structure, Vol.30, pp.1396-1407.
- Fragiacomo**,** M. and Amadio, C., 2003, *Experimental Evaluation of Effective Width in Steel-Concrete Composite Beams*, Journal of Construction Steel Research, Vol.60, pp.199-220.
- Heins, C. P. and Fan, H. M., 1976, *Effective Composite Beam Width at Ultimate Load*, Journal of the Structure Division, Proceedings of the ASCE, Vol.102, pp. 2163-2179.
- Hamoodi, M. J., and Hadi, W. K., 2011, *Tests of Composite Beams with Web Openings*, Engineering and Technology Journal, Vol.29, No.10, pp.2073-2086, Iraq.
- Salama, T. and Nassif, H., 2011, *Effective Flange Width for Composite Steel Beams*, Journal of Engineering Research, Vol.8, No.1, pp.28-43.

Table 1. Effective slab width formulas in various codes.

Code	Formula
AASHTO	**$2\bar{b}$ is least of:** **1. L/4** **2. s** **3. 12hc**
ACI	**$2\bar{b}$ (interior girder) is least of:** **1. L/4** **2. s** **3.bw + 16hc** **$2\bar{b}$ (exterior girder) is least of:** **1. L/12+bw** **2. 6hc+bw** **3. s/2+bw**
AISC	**$2\bar{b}$ is the least of:** **1. L/4** **2. s** **3. 2be**
BSI 8110	**$2\bar{b}$ is least of:** **1. L/5+bw** **2. s**

Where:

(**L)** span length, (**s**) spacing of beams, ($\mathbf{h_c}$) concrete slab thickness, ($\mathbf{b_w}$) width of web for reinforced concrete T-beams, ($\mathbf{b_e}$) distance from beam center to the free edge of the slab.

Table 2. Material properties used for composite steel-concrete beam verification study, **Hamoodi and Hadi, 2011**.

	Symbol	Definition	Value
Concrete	f'_c	Compressive Strength (MPa)	23.20
	E_c	Young's Modulus (MPa)	22540
	f_{ct}	Tensile Strength (MPa)	1.59
	v	Poisson's Ratio	0.15
Reinforcement	f_Y	Yield Stress (MPa)	650
	E_s	Young's Modulus (MPa)	198000
	υ	Poisson's Ratio	0.30
Steel Beam	f_Y	Yield Stress (MPa)	337
	E_s	Young's Modulus (MPa)	196000
	υ	Poisson's Ratio	0.30
Shear Connector	H	Overall Height (mm)	45
	φ	Diameter (mm)	8
	S_{stud}	Spacing (mm)	150
	N_f	Number of Studs per row	15
	E_s	Young's Modulus (MPa)	200000

Table 3. Comparison between experimental and numerical results of beam CB0.

Beam	Load (kN)	Deflection (mm)		Absolute Error %
		Experimental	Analytical	
(CB0)	20	1.2511	1.2467	0.35
	40	2.5321	2.4912	1.6
	60	3.7678	3.8755	2.85
	80	4.9592	4.9838	0.14

Table 4. Comparison between experimental and numerical results of beam CB3.

Beam	Load (kN)	Deflection (mm)		Absolute Error %
		Experimental	Analytical	
(CB3)	20	1.391	1.438	3.38
	40	2.792	2.876	3.10
	60	4.131	4.313	2.85
	80	5.731	5.751	0.348

Table 5. Effective slab width ratio.

Beam Type	Effective Slab Width Ratio $\bar{b}/b$		
	Mid-span		
	CL	LL	UDL
CB0	0.725	0.889	0.951
CB1	0.578	0.858	0.861
CB2	0.593	0.891	0.948
CB3	0.611	0.909	0.930
CB4	0.576	0.855	0.904
CB5	0.580	0.853	0.905

Table 6. Comparison of effective slab width at mid-span with design specifications.

Beam Type	$2\bar{b}$ (mm)			AASHTO	ACI	AISC
	CL	LL	UDL			
CB0	362.286	444.693	475.621	500	500	500
CB1	289.02	429.217	430.545	500	500	500
CB2	296.594	445.473	438.287	500	500	500
CB3	305.426	454.327	465.031	500	500	500
CB4	288.232	427.251	452.225	500	500	500
CB5	289.906	426.560	452.302	500	500	500

Table 7. Effect of panel proportioning on the effective slab width.

Beam Type	Panel (*) Proportion	Effective Slab Width Ratio $\bar{b}/b$		
		Mid-span		
		CL	LL	UDL
CB3	0.25	0.611	0.909	0.930
	0.40	0.602	0.908	0.914
	0.50	0.543	0.885	0.908
CB4	0.25	0.577	0.855	0.905
	0.40	0.548	0.797	0.873
	0.50	0.529	0.770	0.867

(*) Panel proportion = 2b/L, L = 2000mm

Table 8. Comparison of effective slab width at mid-span with design specifications.

Beam Type	Panel (*) Proportion	$2\bar{b}$ (mm)			AASHTO	ACI	AISC
		CL	LL	UDL			
CB3	0.25	305.426	454.327	465.130	500	500	500
	0.40	481.214	727.100	731.223	500	500	500
	0.50	542.874	885.393	935.342	500	500	500
CB4	0.25	288.232	427.251	452.225	500	500	500
	0.40	438.156	637.716	698.748	500	500	500
	0.50	528.760	769.982	867.167	500	500	500

(*) Panel proportion = 2b/L, L = 2000mm

Table 9. Effect of varying slab thickness on the effective slab width ratio.

Beam Type	Slab Thickness(mm)	Effective Slab Width Ratio $\bar{b}/b$		
		Mid-span		
		CL	LL	UDL
CB3	60	0.611	0.909	0.930
	90	0.613	0.847	0.945
	120	0.606	0.815	0.930
CB4	60	0.577	0.855	0.905
	90	0.600	0.879	0.927
	120	0.602	0.890	0.939

Table 10. Comparison of effective slab width with design specifications for different values of slab thickness.

Beam Type	Slab Thickness(mm)	$2\bar{b}$ (mm)			AASHTTO	ACI	AISC
		CL	LL	UDL			
CB3	60	305.426	454.327	465.130	500	500	500
	90	306.566	454.446	472.731	500	500	500
	120	303.112	407.583	475.376	500	500	500
CB4	60	288.232	427.251	452.225	500	500	500
	90	299.916	439.604	463.705	500	500	500
	120	301.200	444.992	469.596	500	500	500

Table 11. Effect of slab boundary conditions on the effective width ratio.

Beam Type	Panel Proportion	Effective Slab Width Ratio Ratio $\bar{b}/b$					
		Mid-span					
		Continues Slab			Discontinues Slab		
		CL	LL	UDL	CL	LL	UDL
CB3	0.25	0.613	0.910	0.931	0.611	0.847	0.930
	0.40	0.588	0.912	0.910	0.602	0.908	0.914
	0.50	0.548	0.896	0.925	0.543	0.885	0.935
CB4	0.25	0.578	0.855	0.909	0.577	0.855	0.905
	0.40	0.535	0.799	0.878	0.548	0.797	0.873
	0.50	0.518	0.777	0.880	0.529	0.770	0.867

Table 12. Comparison of effective slab width at mid-span with design specifications.

Beam Type	Panel Proportion	$2\bar{b}$ (mm)			AASHTTO	ACI	AISC
		CL	LL	UDL			
CB3	0.25	306.451	454.844	464.928	500	500	500
	0.40	470.290	729.235	728.036	500	500	500
	0.50	547.811	895.587	924.898	500	500	500
CB4	0.25	289.185	427.286	454.356	500	500	500
	0.40	407.615	638.822	702.552	500	500	500
	0.50	457.871	776.699	880.362	500	500	500

Table 13. Effect of steel beam depth on the effective slab width.

Beam Type	Steel Beam Depth (mm)	Effective Slab Width Ratio $\bar{b}/b$		
		Mid-span		
		CL	LL	UDL
CB3	160	0.611	0.909	0.930
	200	0.564	0.893	0.926
	240	0.527	0.879	0.920
CB4	160	0.577	0.855	0.905
	200	0.537	0.833	0.898
	240	0.512	0.820	0.903

Table 14. Comparison of effective slab width with design specifications for different values of steel beam depth.

Beam Type	Steel Beam Depth mm)	$2\bar{b}$ (mm)			AASHTTO	ACI	AISC
		CL	LL	UDL			
CB3	160	305.426	454.327	465.130	500	500	500
	200	282.219	446.745	463.013	500	500	500
	240	263.635	439.604	460.266	500	500	500
CB4	160	288.232	427.251	452.225	500	500	500
	200	268.517	416.249	448.992	500	500	500
	240	256	410.143	451.514	500	500	500

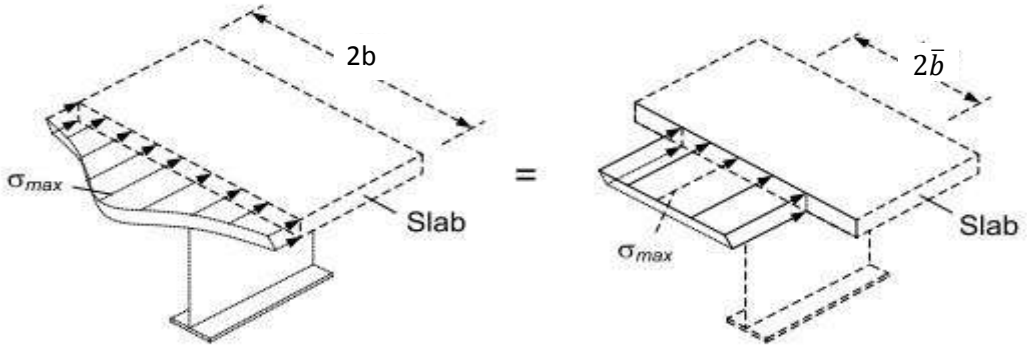

Figure 1. Shear lag effect.

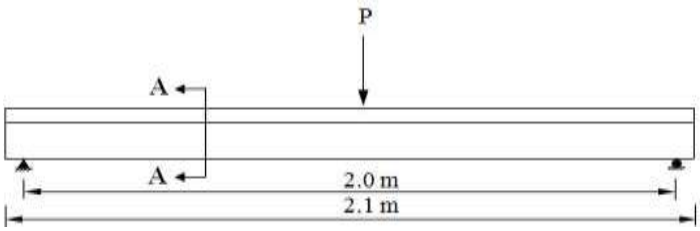

(a) Typical dimensions of a composite beam.

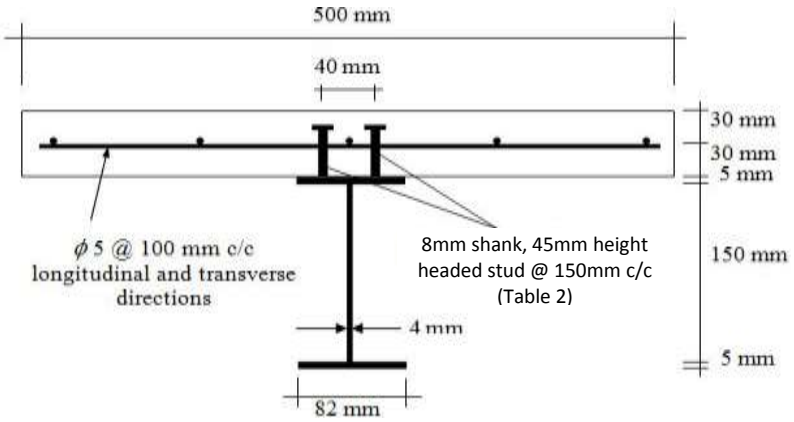

(b) Section A-A.

Figure 2. Typical cross section of the composite beam, **Hamoodi and Hadi, 2011**.

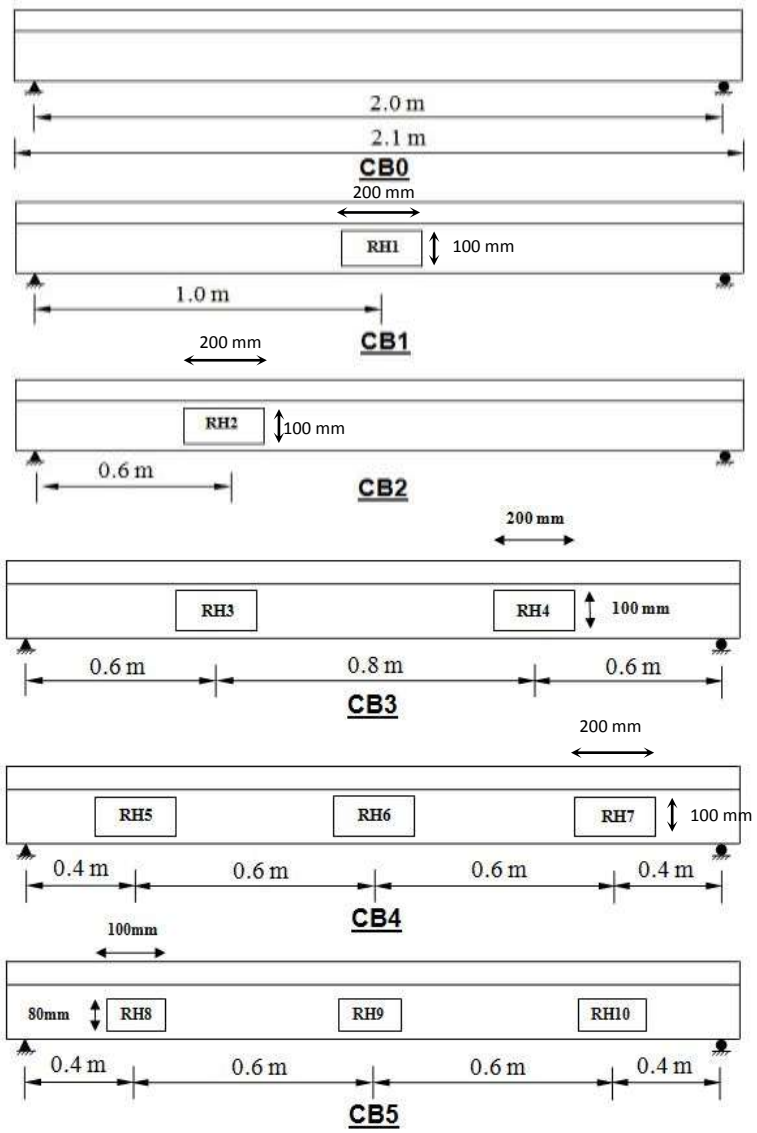

Figure 3. Configurations and locations of web openings, **Hamoodi and Hadi, 2011**.

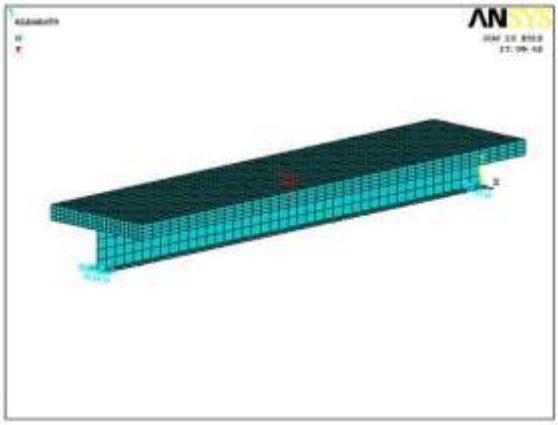

Figure 4. Three-Dimensional finite element mesh for the composite beam CB0.

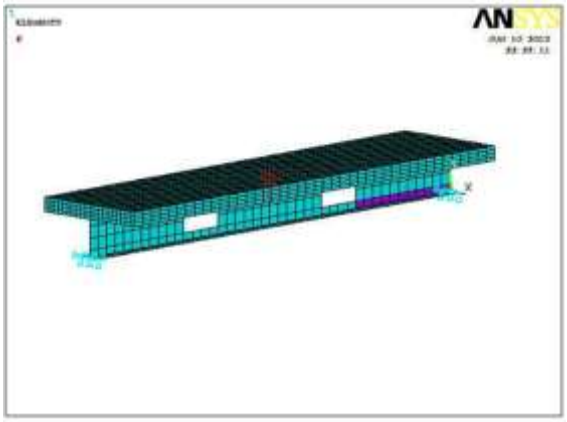

Figure 5. Three-dimensional finite element mesh for composite beam CB3.

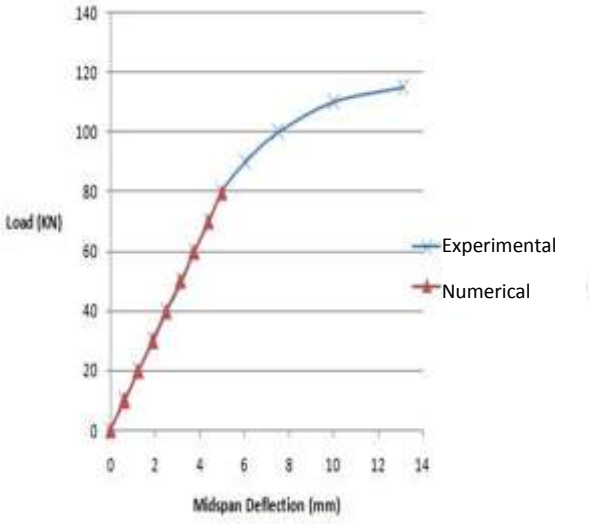

Figure 6. Experimental and numerical load- deflection curve for beam CB0.

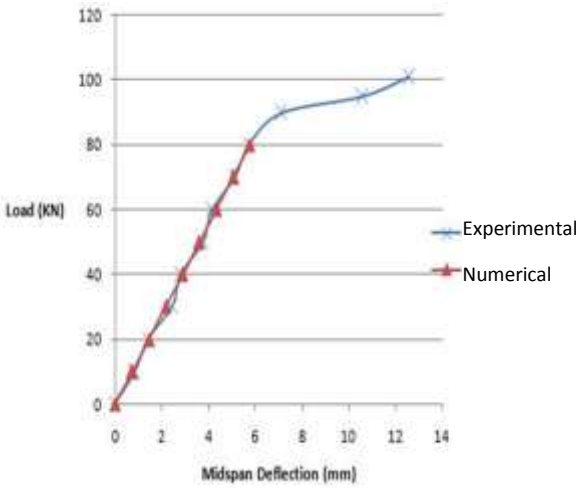

Figure 7. Experimental and numerical load-deflection curve for beam CB3.

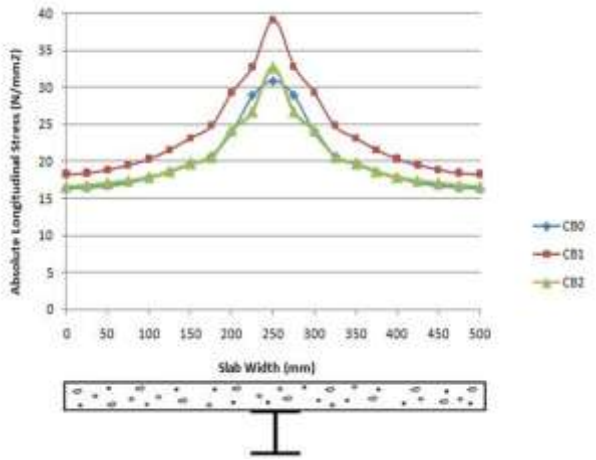

Figure 8. Slab stress distributions of beams CB0, CB1 and CB2 due to (CL) loading.

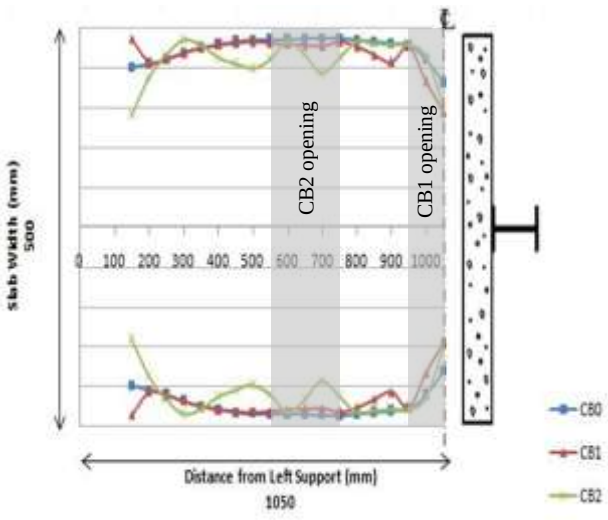

Figure 9. Effective slab width of beams CB0, CB1, and CB2 due to (CL) loading.

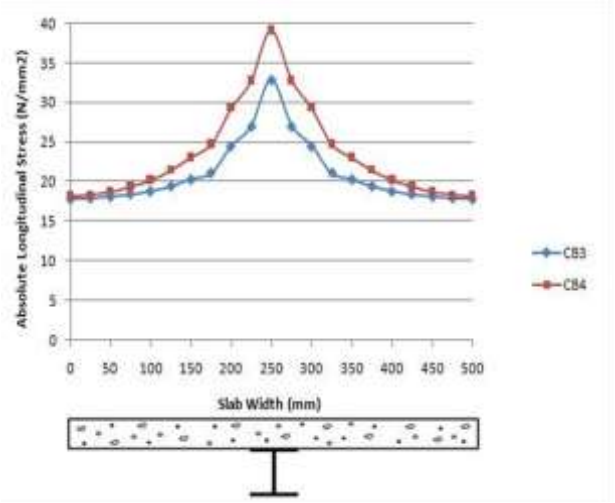

Figure 10. Slab stress distribution at mid-span of CB3 and CB4 beams due to (CL) loading.

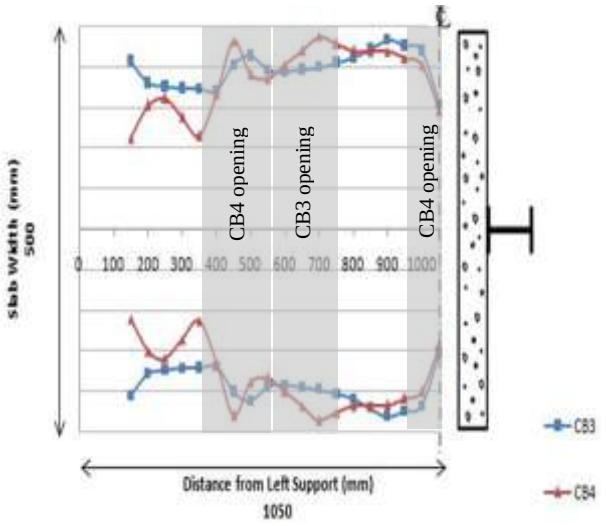

Figure 11. Effective slab width of beams CB3 and CB4 due to (CL) loading.

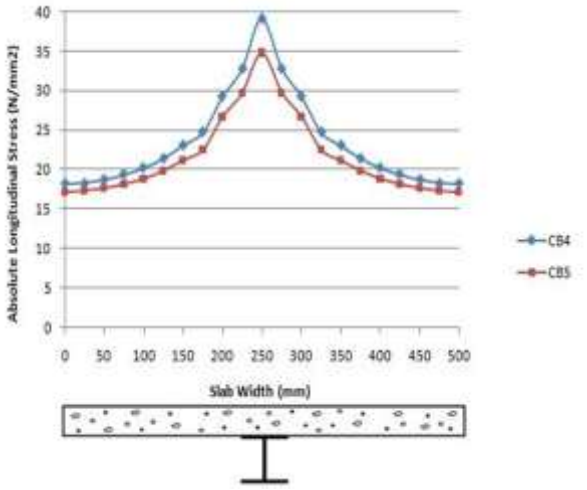

Figure 12. Slab stress distribution at mid-Span of CB4 and CB5 Beams Due to (CL) Loading.

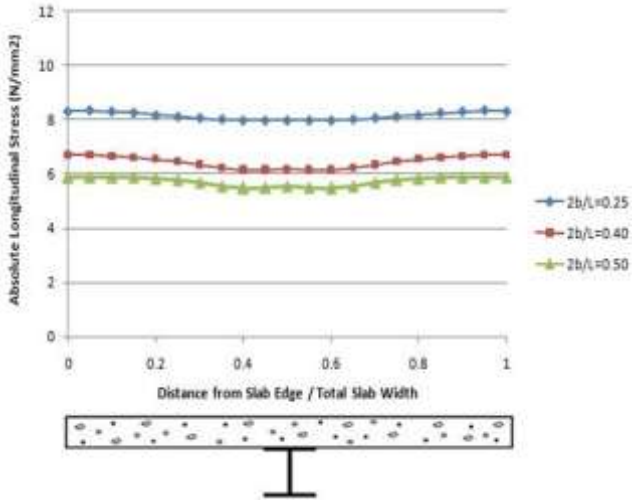

Figure 13. Slab stress distribution of CB3 for various panel proportions due to (UDL) loading.

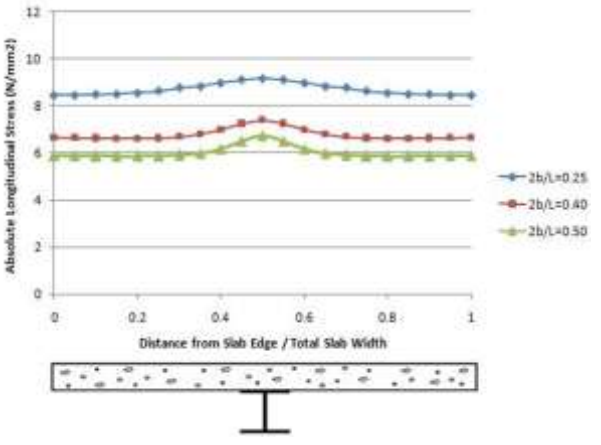

Figure 14. Slab stress distribution of CB4 for various panel proportions due to (UDL) loading.

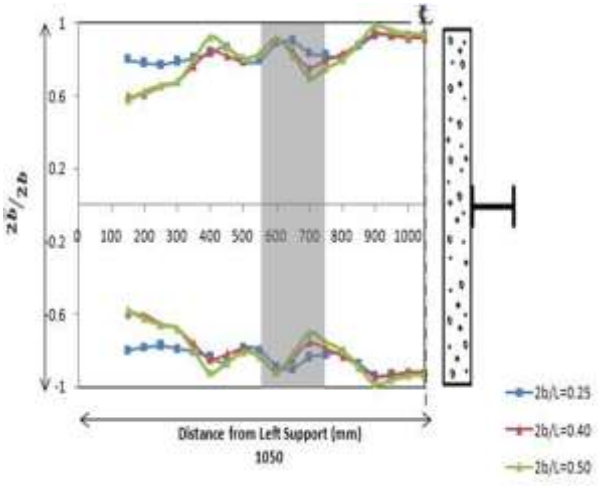

Figure 15. Effective slab width for CB3 for various panel proportions due to (UDL) loading.

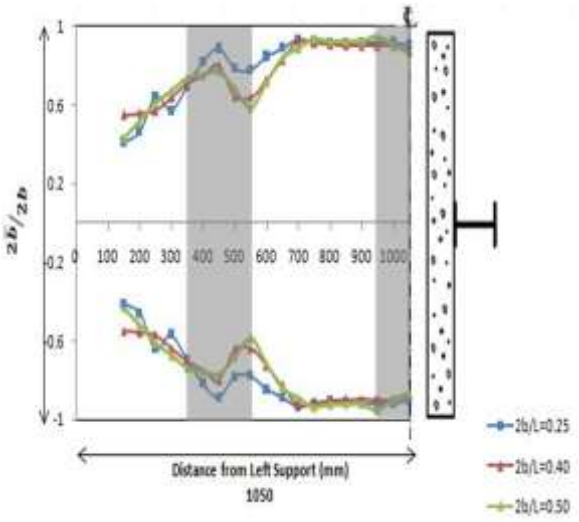

Figure 16. Effective slab width for CB4 for various panel proportions due to (UDL) loading.

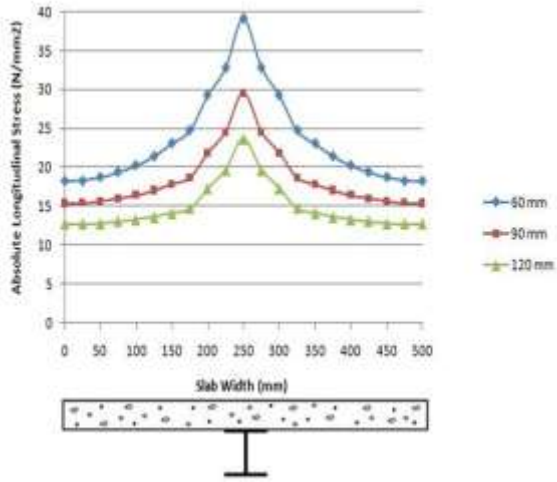

Figure 18. Slab stress distribution of CB4 for various slab thicknesses due to (CL) loading.

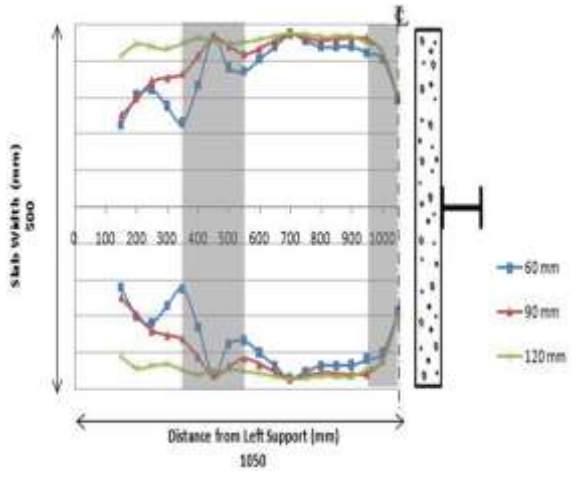

Figure 20. Effective slab width for CB4 for various slab thicknesses due to (CL) loading.

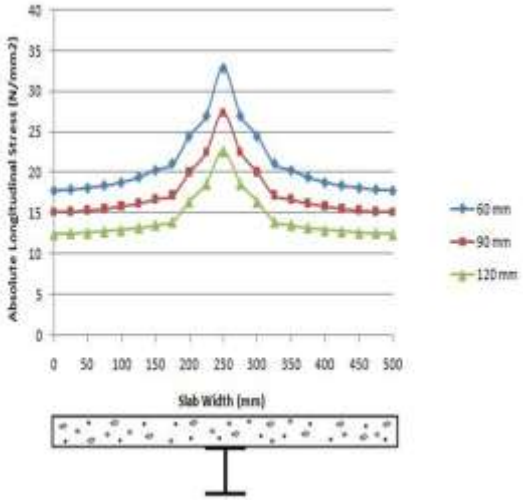

Figure 17. Slab stress distribution of CB3 for various slab thicknesses due to (CL) loading.

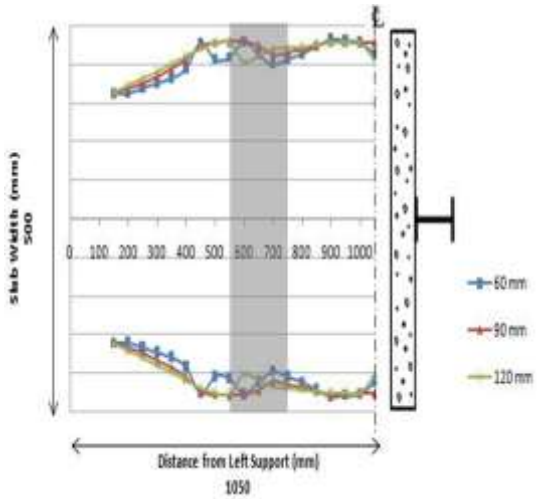

Figure 19. Effective slab width for CB3 for various slab thicknesses due to (LL) loading.

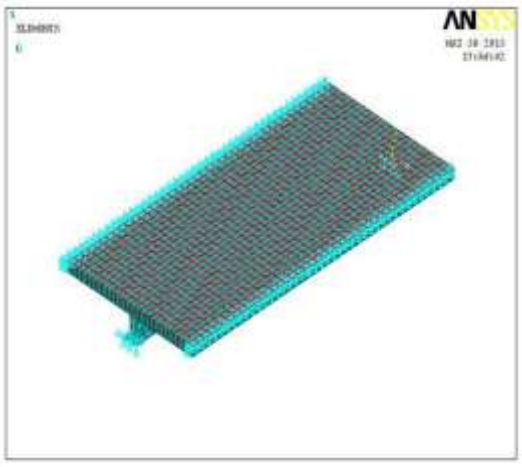

Figure 21. Boundary conditions modeling adopted to simulate concrete slab continuity.

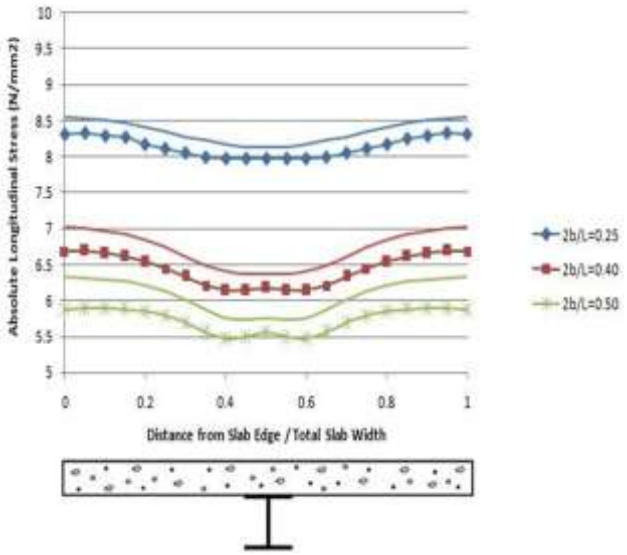

Figure 22. Slab stress distribution for CB3 for discontinuous slab (marked line) and continuous slab (unmarked line) due to (UDL) loading.

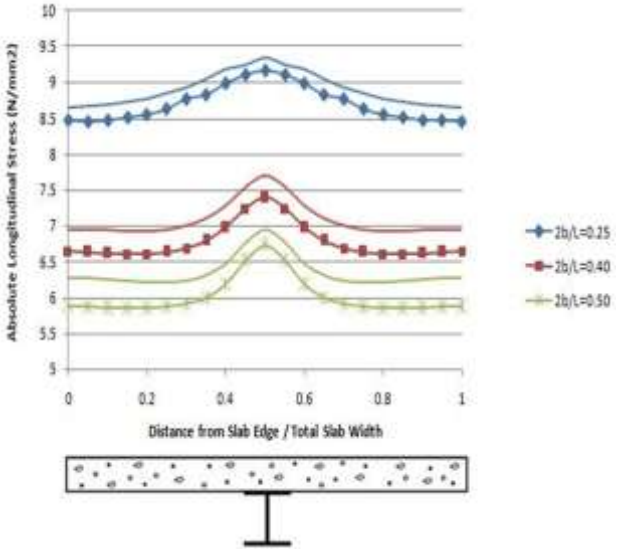

Figure 23. Slab stress distribution for CB4 for discontinuous slab (marked line) and continuous slab (unmarked line) due to (UDL) loading.

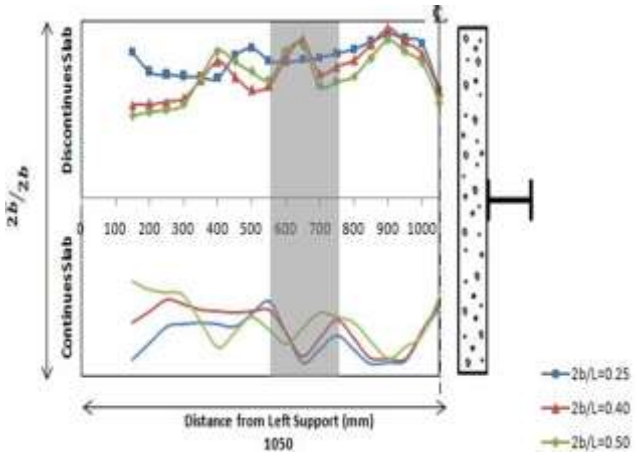

Figure 24. Slab stress distribution for CB3 for discontinuous slab (marked line) and continuous slab (unmarked line) due to (CL) Loading.

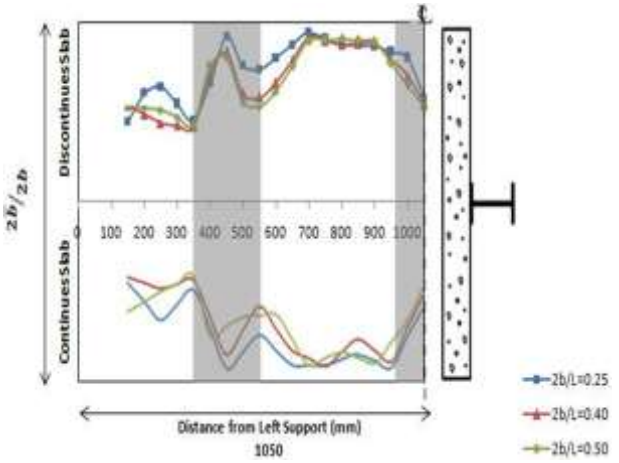

Figure 25. Slab stress distribution for CB4 for discontinuous slab (marked line) and continuous slab (unmarked line) due to (CL) Loading.

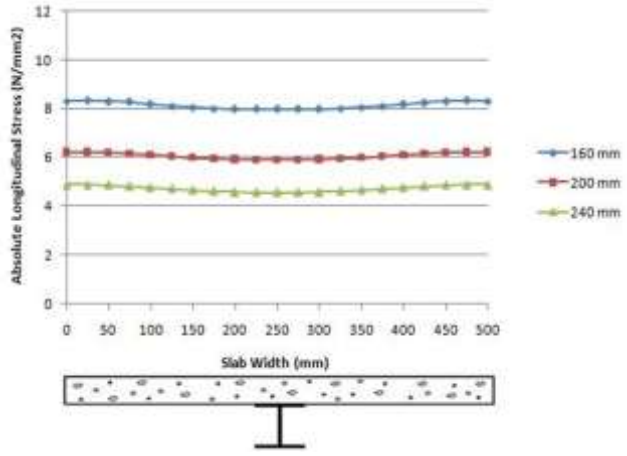

Figure 26. Slab stress distribution of beam CB3 for various steel beam depths due to (UDL) loading.

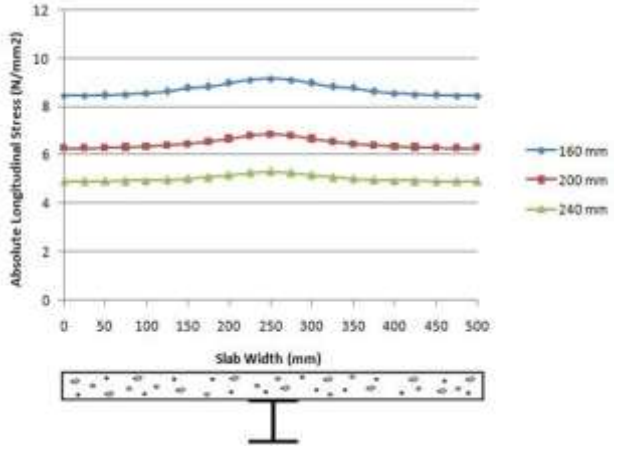

Figure 27. Slab stress distribution of beam CB4 for various steel beam depths due to (UDL) loading.

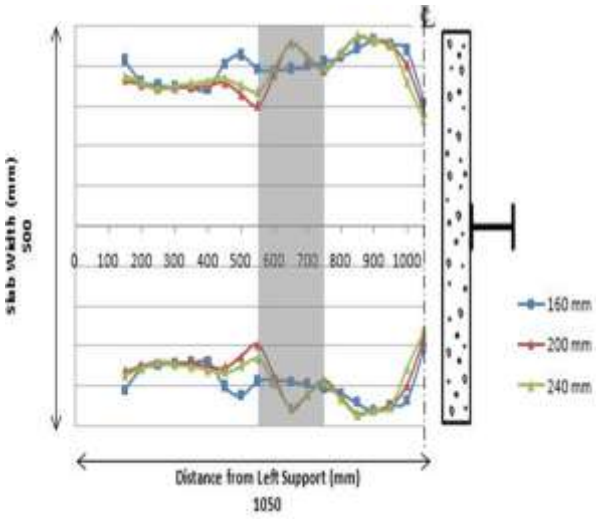

Figure 28. Effective slab width for CB3 for various steel beam depths due to (CL) loading.

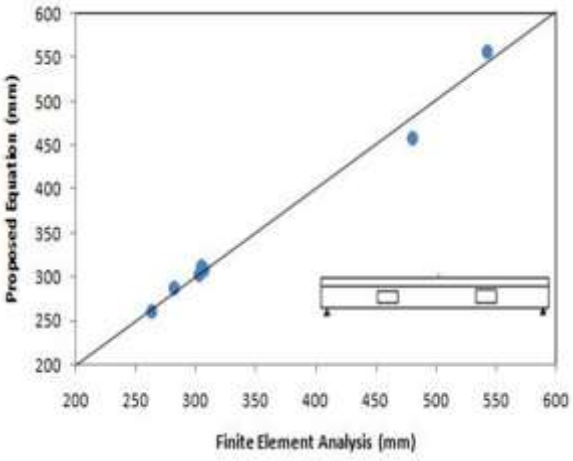

Figure 30. Effective slab width obtained from FEA and proposed equation (2) for beam CB3 due to concentrated load.

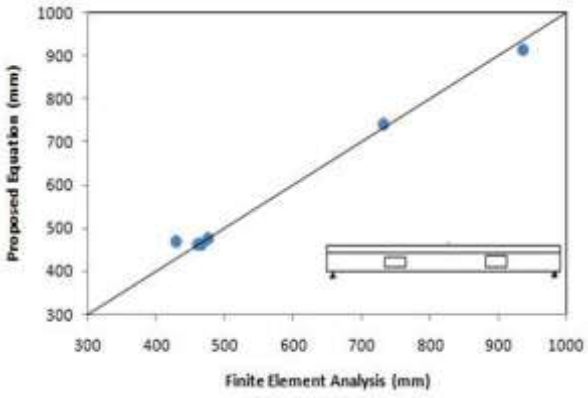

Figure 32. Effective slab width obtained from FEA and proposed equation (3) for beam CB3 due to uniformly distributed load.

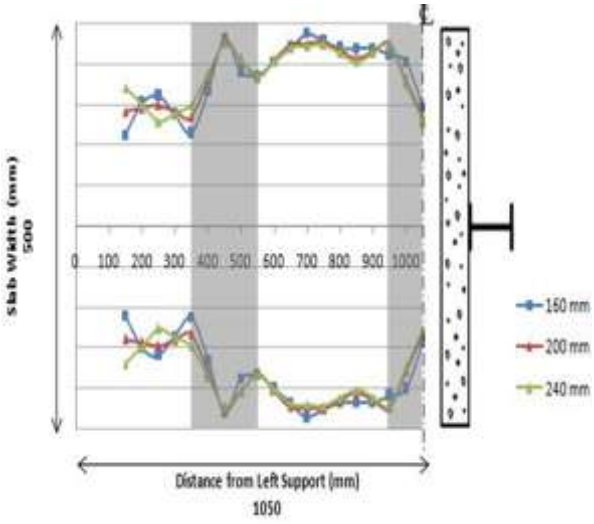

Figure 29. Effective slab width for CB4 for various steel beam depths due to (CL) loading.

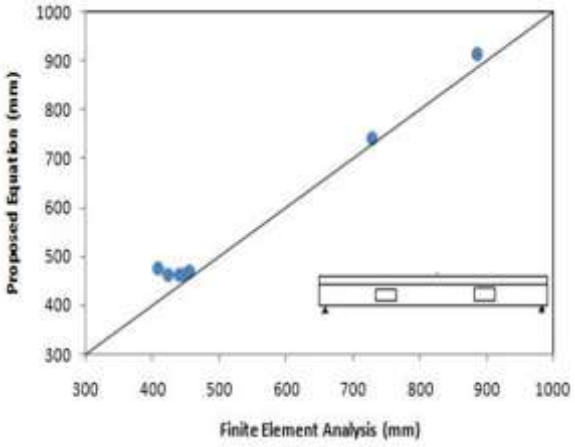

Figure 31. Effective slab width obtained from FEA and proposed equation (3) for beam CB3 due to concentrated load.

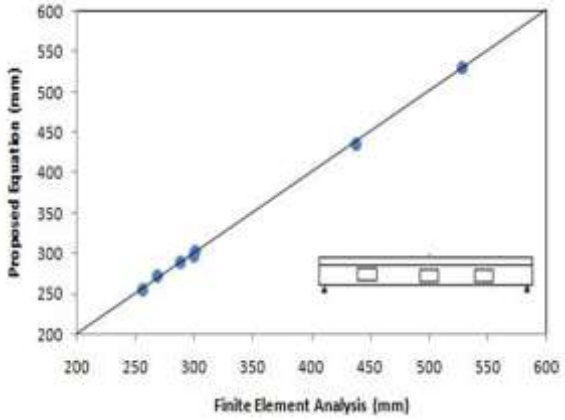

Figure 33. Effective slab width obtained from FEA and proposed equation (4) for beam CB4 due to uniformly distributed load.

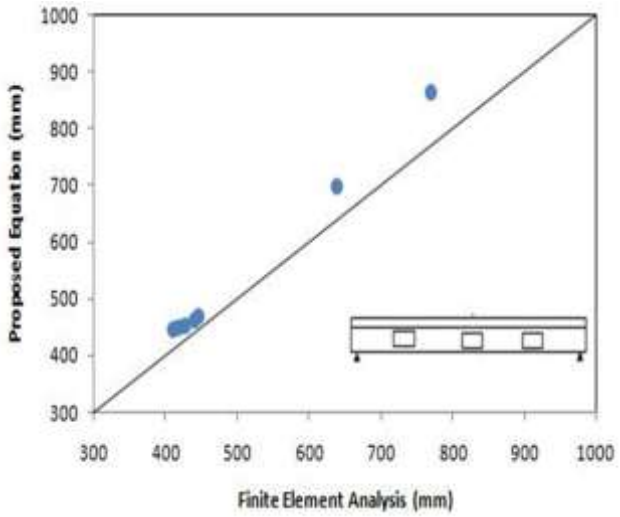

Figure 34. Effective slab width obtained from FEA and proposed equation (5) for beam CB4 due to line load.

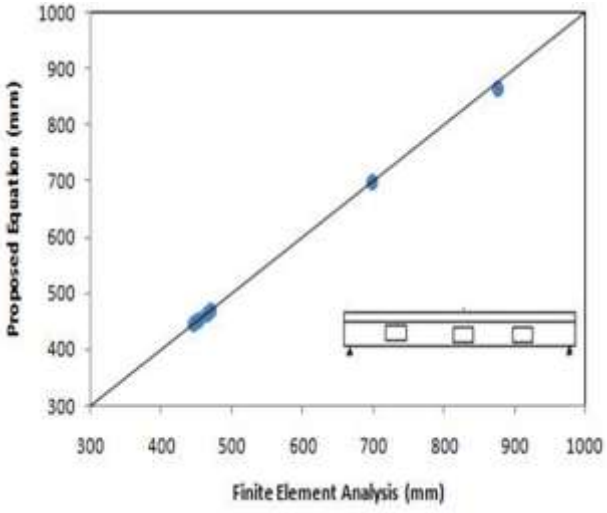

Figure 35. Effective slab width obtained from FEA and proposed equation (5) for beam CB4 due to uniformly distributed load.

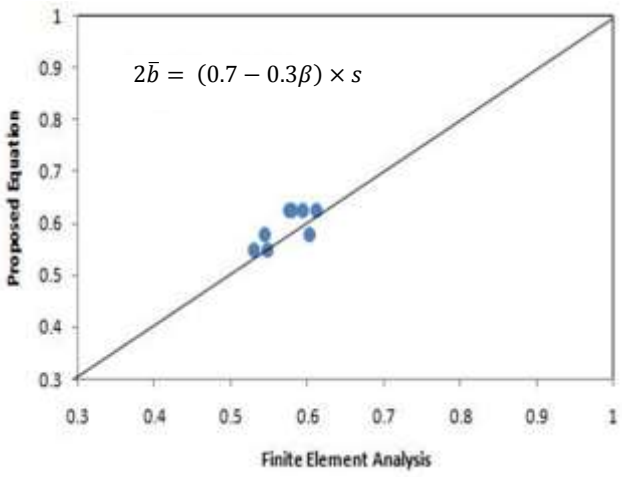

Figure 36. Effective slab width obtained from FEA and simplified equation (6) for beam CB4 due to concentrated load.

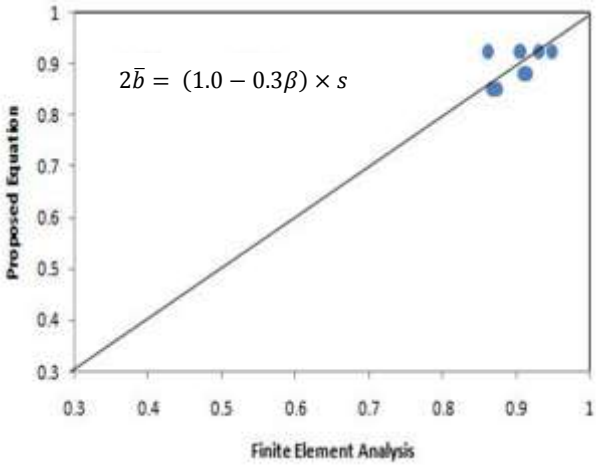

Figure 37. Effective slab width obtained from FEA and simplified equation (7) for beam CB4 due to uniformly distributed load.